Science Advances
AAAS

advances.sciencemag.org/cgi/content/full/5/1/eaau9223/DC1

Supplementary Materials for

Multiplexed enrichment and genomic profiling of peripheral blood cells reveal subset-specific immune signatures

Miguel Reyes, Dwayne Vickers, Kianna Billman, Thomas Eisenhaure, Paul Hoover, Edward P. Browne, Deepak A. Rao, Nir Hacohen*, Paul C. Blainey*

*Corresponding author. Email: nhacohen@broadinstitute.org (N.H.); pblainey@broadinstitute.org (P.C.B.)

Published 25 January 2019, *Sci. Adv.* **5**, eaau9223 (2019)
DOI: 10.1126/sciadv.aau9223

The PDF file includes:

Fig. S1. Detailed schematic of integrated workflow implemented on microfluidic chip.
Fig. S2. Flow cytometry gating strategy.
Fig. S3. Chip sorting optimization and comparison with benchtop magnetic isolation.
Fig. S4. Representative Bioanalyzer traces for conventional benchtop and microfluidic device whole transcriptome amplicons (WTA) for four different lysate samples from the four indicated FACS-sorted cell subsets.
Fig. S5. Differential gene expression analysis between microfluidic and benchtop RNA-seq libraries.
Fig. S6. Chip enrichment validation by gene expression profiles.
Fig. S7. Comparison between conventional and device-processed RNA-seq libraries (full workflow).
Fig. S8. RNA-seq correlation plots for in vitro–treated PBMCs.
Fig. S9. Gene set enrichment analysis (Reactome sets) comparing treated PBMCs versus control.
Fig. S10. Volcano plots showing differentially expressed genes between patients with SLE and matched healthy controls for four different subsets.
Fig. S11. Heat map showing relative IFN-signature scores across different cell types of 10 patients.
Supplementary Note
Supplementary Methods

Other Supplementary Material for this manuscript includes the following:

(available at advances.sciencemag.org/cgi/content/full/5/1/eaau9223/DC1)

Table S1 (Microsoft excel format). Ex vivo treatment differential expression (DE) results.

Table S2 (Microsoft excel format). Patient information for clinical study.
Table S3 (Microsoft excel format). SLE DE and gene set enrichment analysis results.
Data file S1 (.dwg format). Device design.
Data file S2 (.zip format). Gene expression matrices.

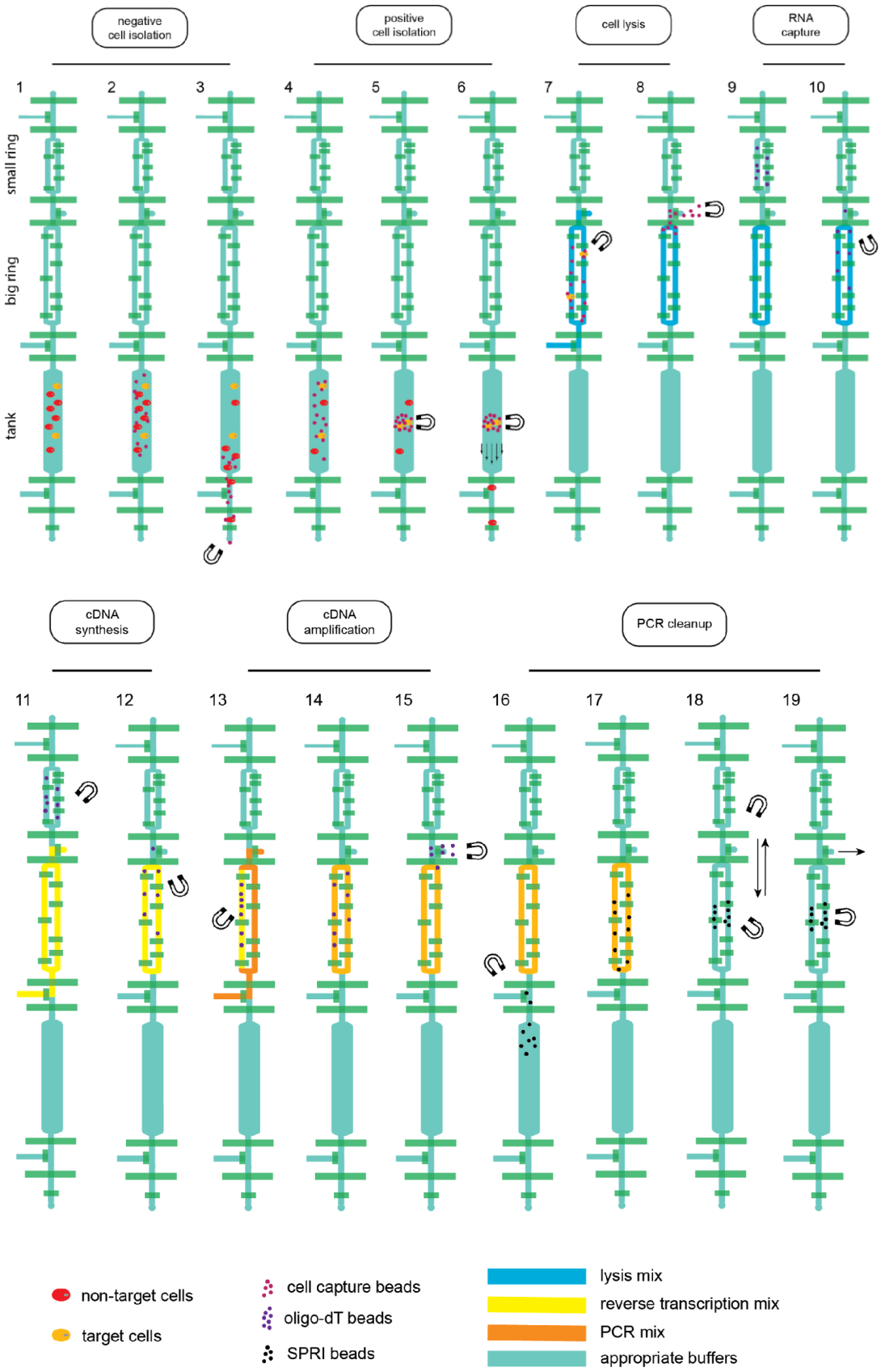
negative cell isolation
positive cell isolation
cell lysis
RNA capture
1
2
3
4
5
6
7
8
9
10
small ring
big ring
tank
cDNA synthesis
cDNA amplification
PCR cleanup
11
12
13
14
15
16
17
18
19
non-target cells
target cells
cell capture beads
oligo-dT beads
SPRI beads
lysis mix
reverse transcription mix
PCR mix
appropriate buffers

Fig. S1. Detailed schematic of integrated workflow implemented on microfluidic chip. Cell sorting is conducted using at least one of the following modular steps, or combinations of these steps: (1-3) depletion of non-target cells and (4-6) bead capture of target cells. A permanent magnet is used to either remove non-target cells from the chip (3) or retain them in the tank during washes (6). After sorting, further operations can be implemented for cell lysis and processing of nucleic acids, e.g. sample preparation steps required prior to analysis by NGS. For example, in our RNA-seq protocol, bead-bound target cells are transferred and incubated in the big ring pre-filled with lysis buffer (7). Cell capture beads are then removed (8) and custom oligo-dT beads are loaded through the small ring (9). The oligo-dT beads are moved into the big ring to capture mRNA from the cell lysates (10). The beads are then moved back to the small ring for holding while the big ring is loaded with reverse transcription mix (11). After loading, the beads are brought into the big ring and re-suspended (12). The chip is then transferred to a flat-top thermocycler for the RT reaction. When the reaction finishes, half of the big ring is loaded with PCR mix (13), and the two fluids are mixed together for PCR (14). After which, the beads are removed (15) and SPRI beads are loaded through the tank (16). The beads are incubated with the PCR product (17) and subsequently washed with ethanol (18). Finally, the products are eluted in TE buffer and unloaded from the chip for transposase-driven fragmentation and adaptation (19).

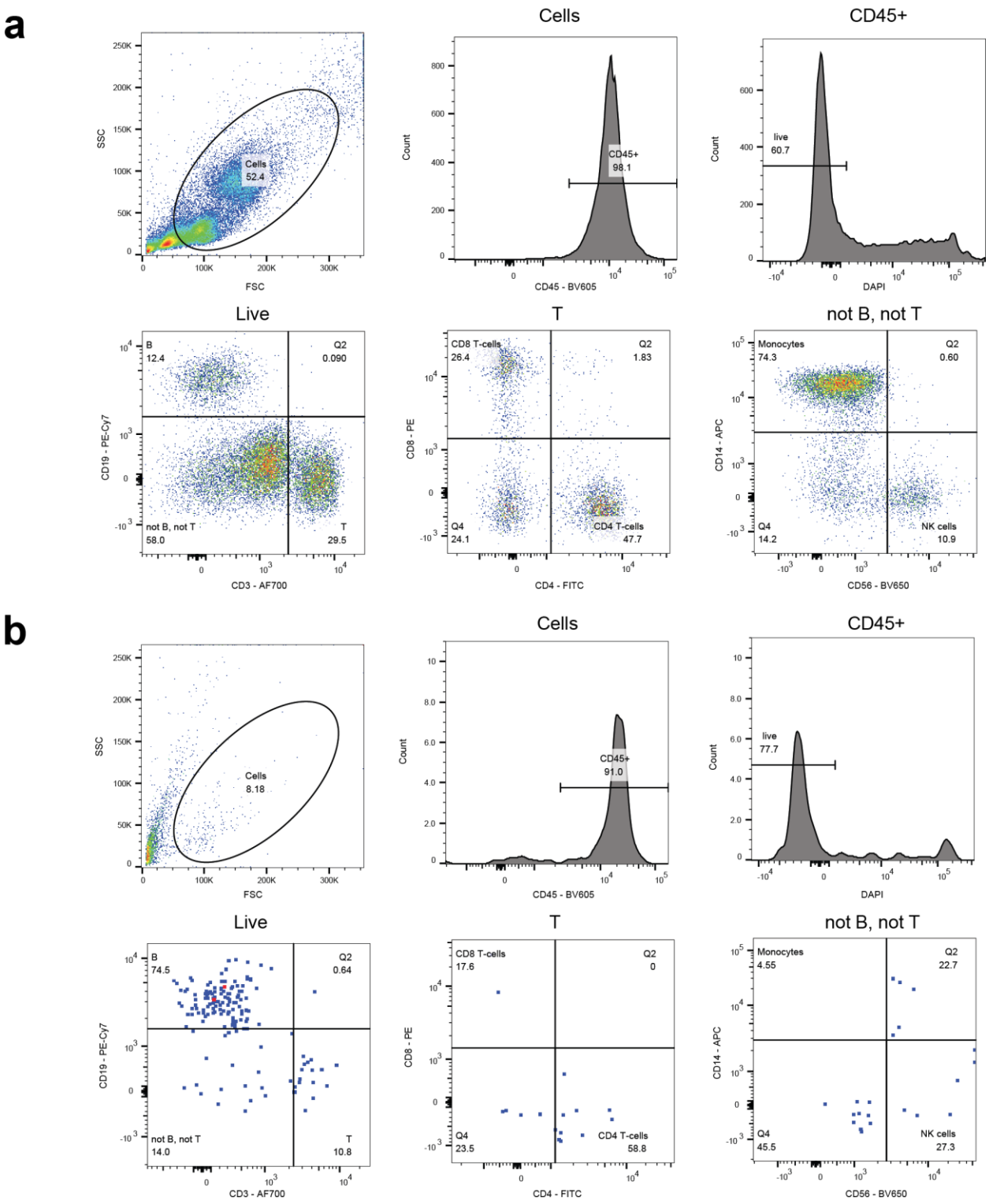

Fig. S2. Flow cytometry gating strategy. Sample flow cytometry gating strategy for quantifying the purity of input (**a**, 1 M cells) or a cell subset (B cells/CD19 shown) sorted using the microfluidic device (**b**, 5000 cells).

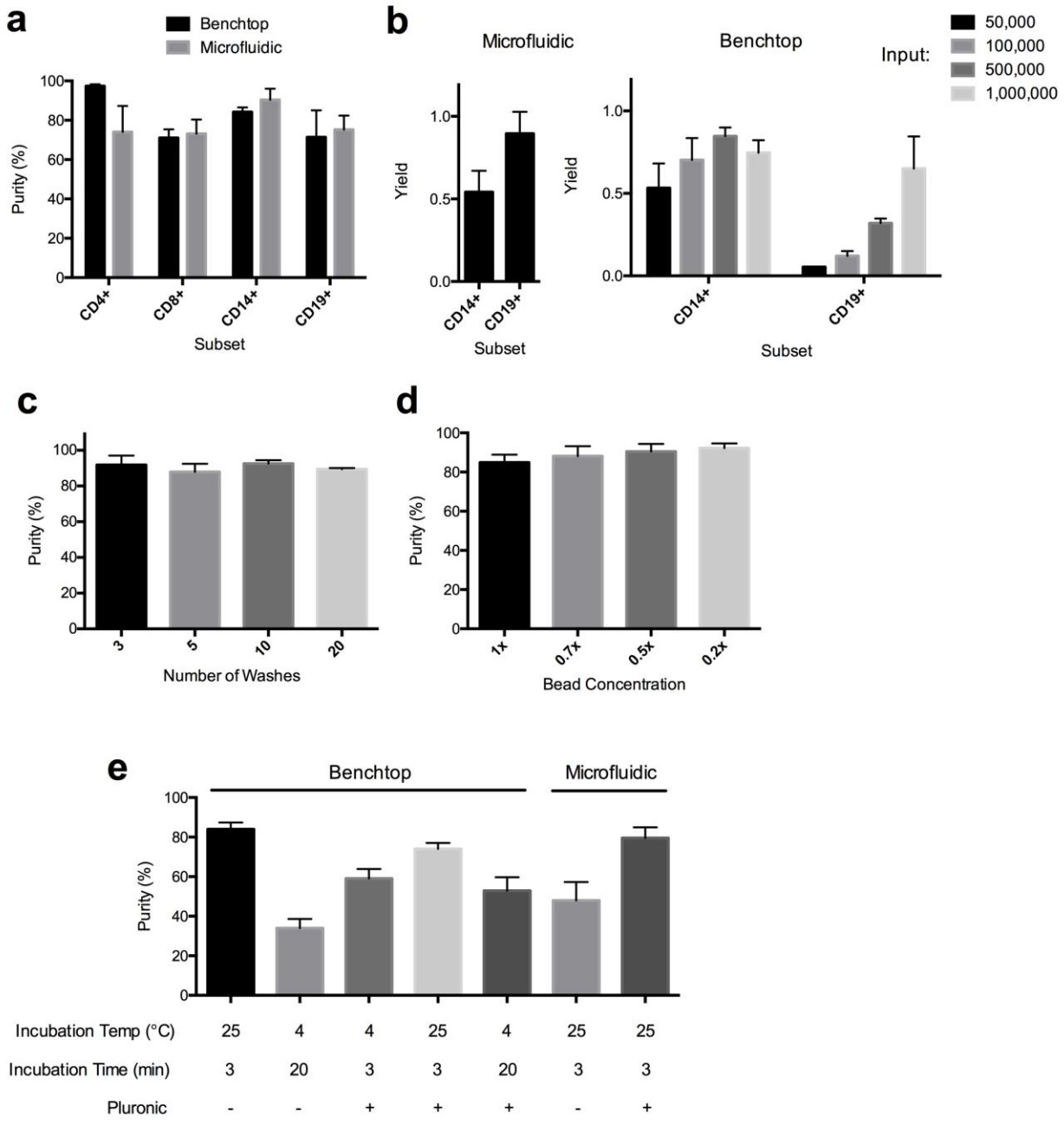

Fig. S3. Chip sorting optimization and comparison with benchtop magnetic isolation. (**a**) Comparison of purity between benchtop and device positive isolation for CD4, CD8, CD14, and CD19. Input cells: 50,000 for microfluidic and 1M for benchtop (following manufacturer's protocols) (**b**) Comparison of yield between benchtop and device positive isolation for CD14 and CD19 with varying amount of input cells for benchtop (**c**, **d**) Sort purity from positive isolation of B cells with varying capture bead concentration and washes. (**e**) Purity obtained from negative isolation of T-cells, with varying incubation and buffer conditions. All error bars indicated S.D., n=2.

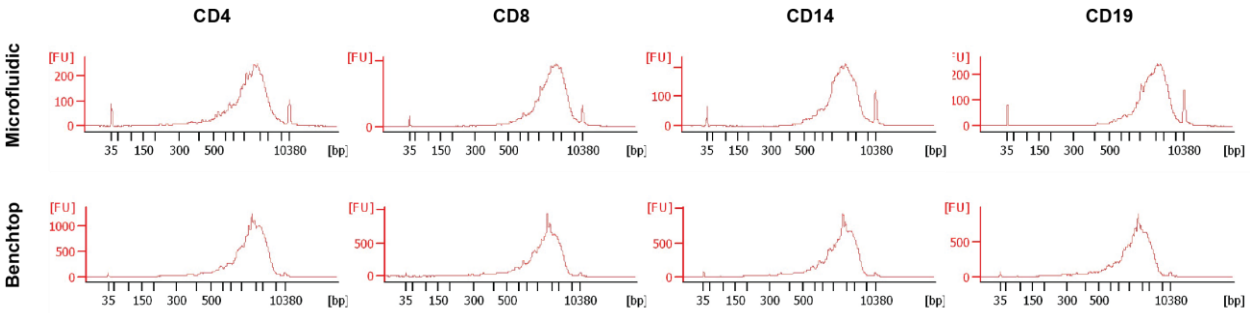

Fig. S4. Representative Bioanalyzer traces for conventional benchtop and microfluidic device whole transcriptome amplicons (WTA) for four different lysate samples from the four indicated FACS-sorted cell subsets.

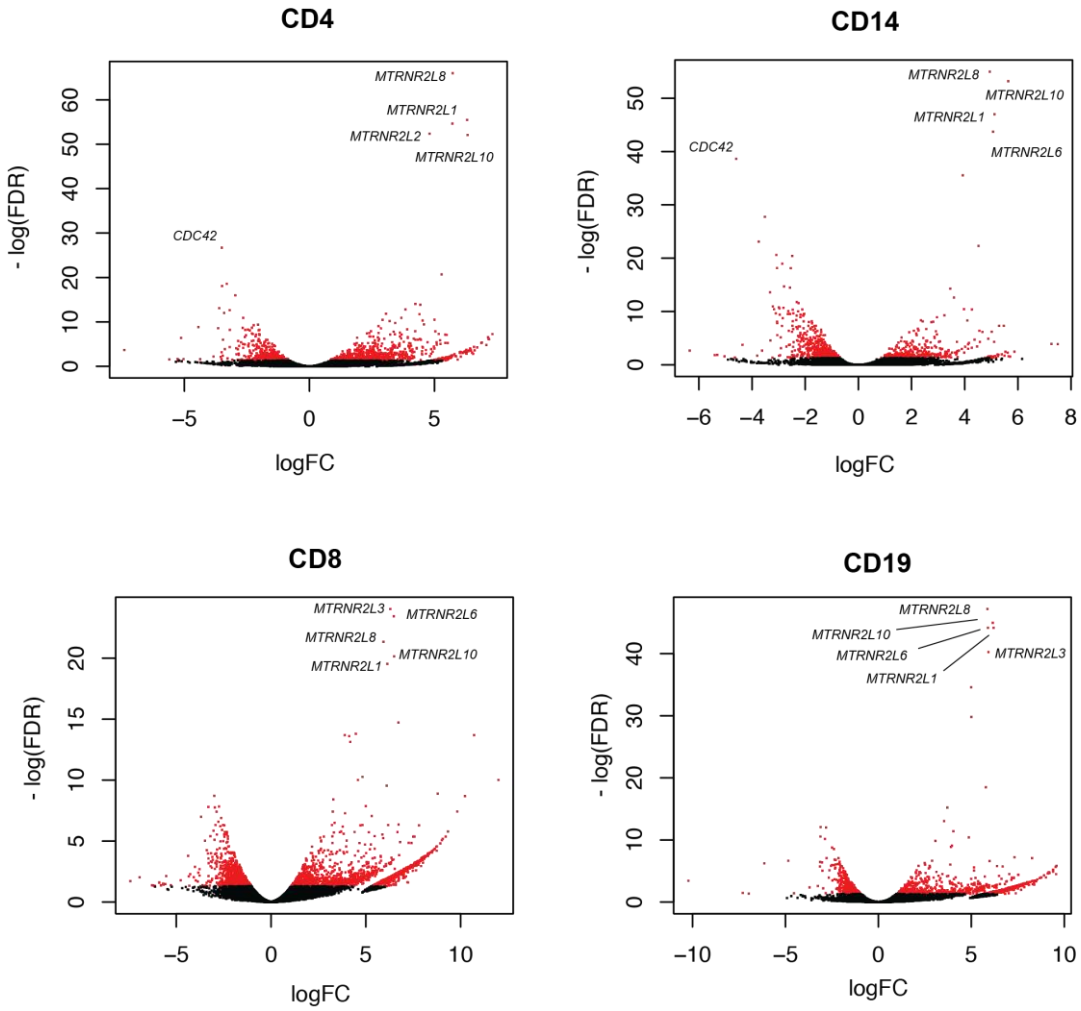

Fig. S5. Differential gene expression analysis between microfluidic and benchtop RNA-seq libraries. Positive fold-change indicates that the gene has higher expression in the benchtop-prepared library. Red points indicate significant differentially expressed genes (FDR < 0.05). Top 5 differentially expressed genes (lowest FDR-corrected *P*) for each subset are labelled.

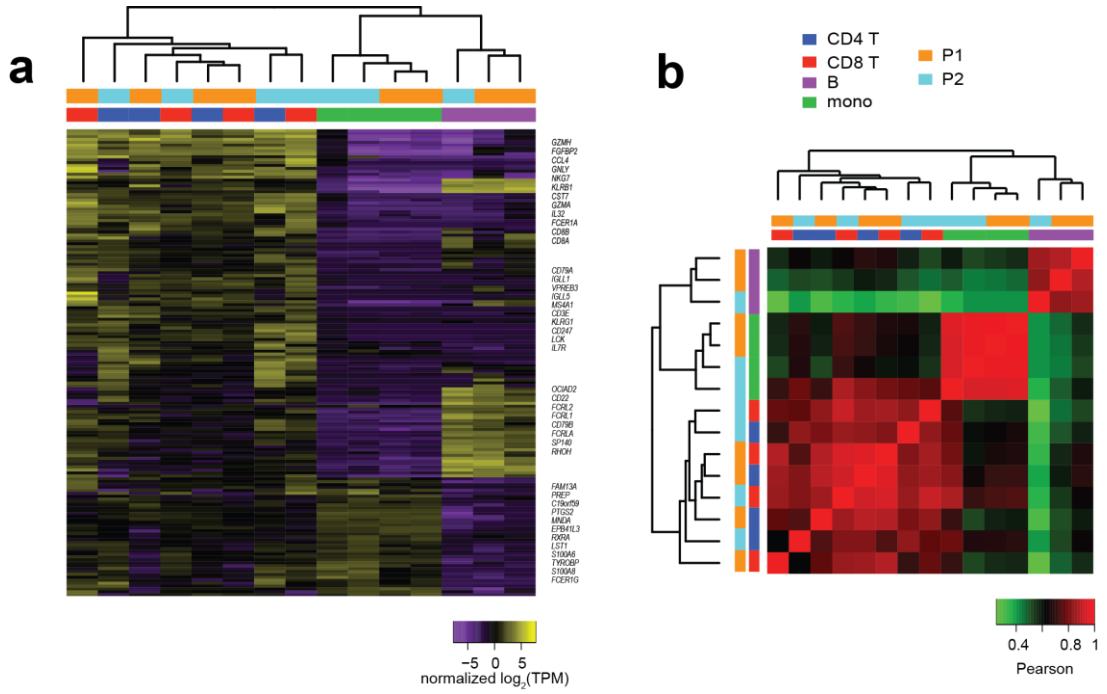

Fig. S6. Chip enrichment validation by gene expression profiles. Healthy PBMCs are sorted and processed in the microfluidic workflow, isolating $CD4^+$ T cells, $CD8^+$ T cells, B cells, and monocytes for two healthy controls. Heatmap (**a**) shows expression levels of significant differentially expressed genes (FDR < 0.05) between all pairwise comparisons between the four cell subsets. Heatmap (**b**) shows Pearson correlation between samples based on differentially expressed genes.

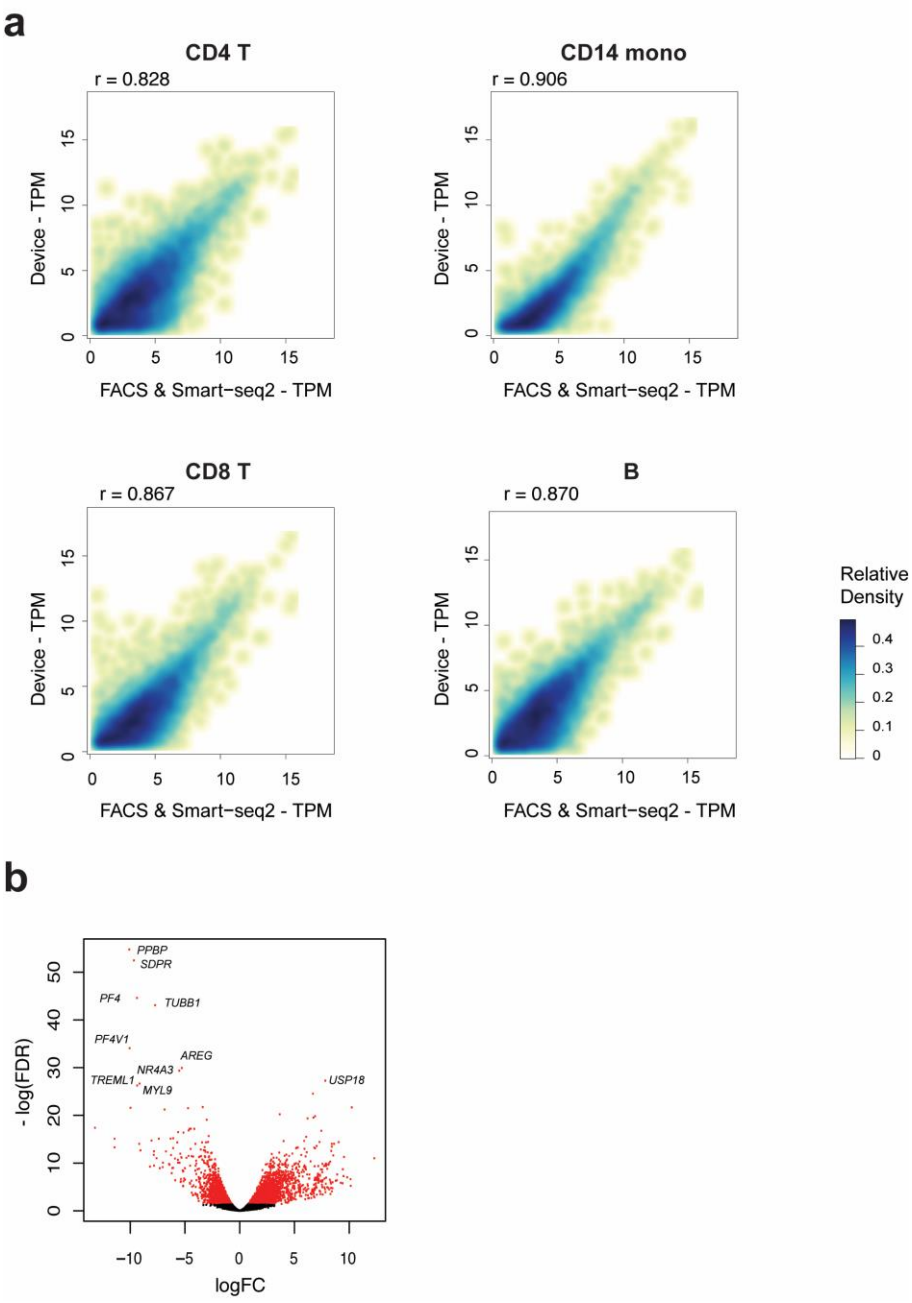

Fig. S7. Comparison between conventional and device-processed RNA-seq libraries (full workflow). (**a**) Scatterplots showing expression levels (TPM, transcripts-per-million) between conventional (FACS & Smart-seq2) and device-processed (device MACS & device RNA-seq) libraries across the four cell subsets. (**b**) Volcano plot showing differentially expression genes between all device-processed and conventional libraries. Positive fold-change indicates that the gene has higher expression in the conventional library. Red points indicate significant differentially expressed genes (FDR < 0.05). Top 10 differentially expressed genes are not from a specific population of immune cells, and are either housekeeping genes (TBB, NR4A3), or from platelets and red blood cells (SDPR, PPBP, HBB, PF4, PF4V1).

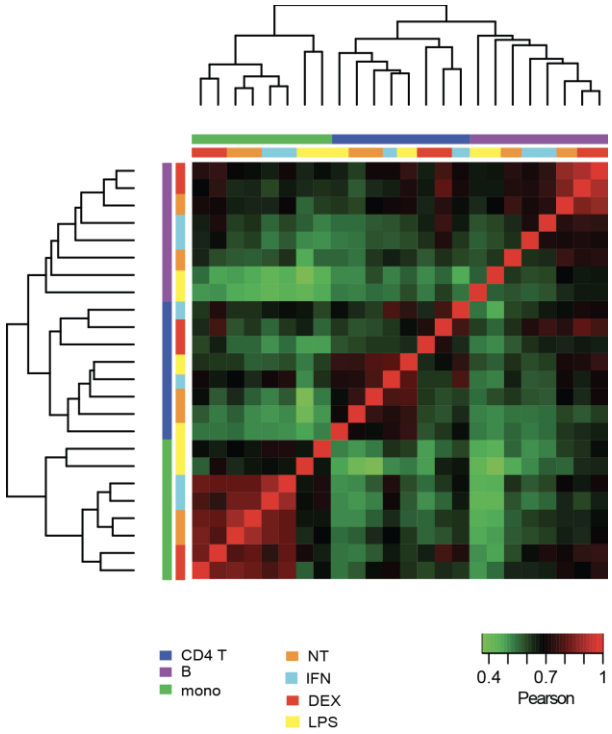

Fig. S8. RNA-seq correlation plots for in vitro–treated PBMCs.

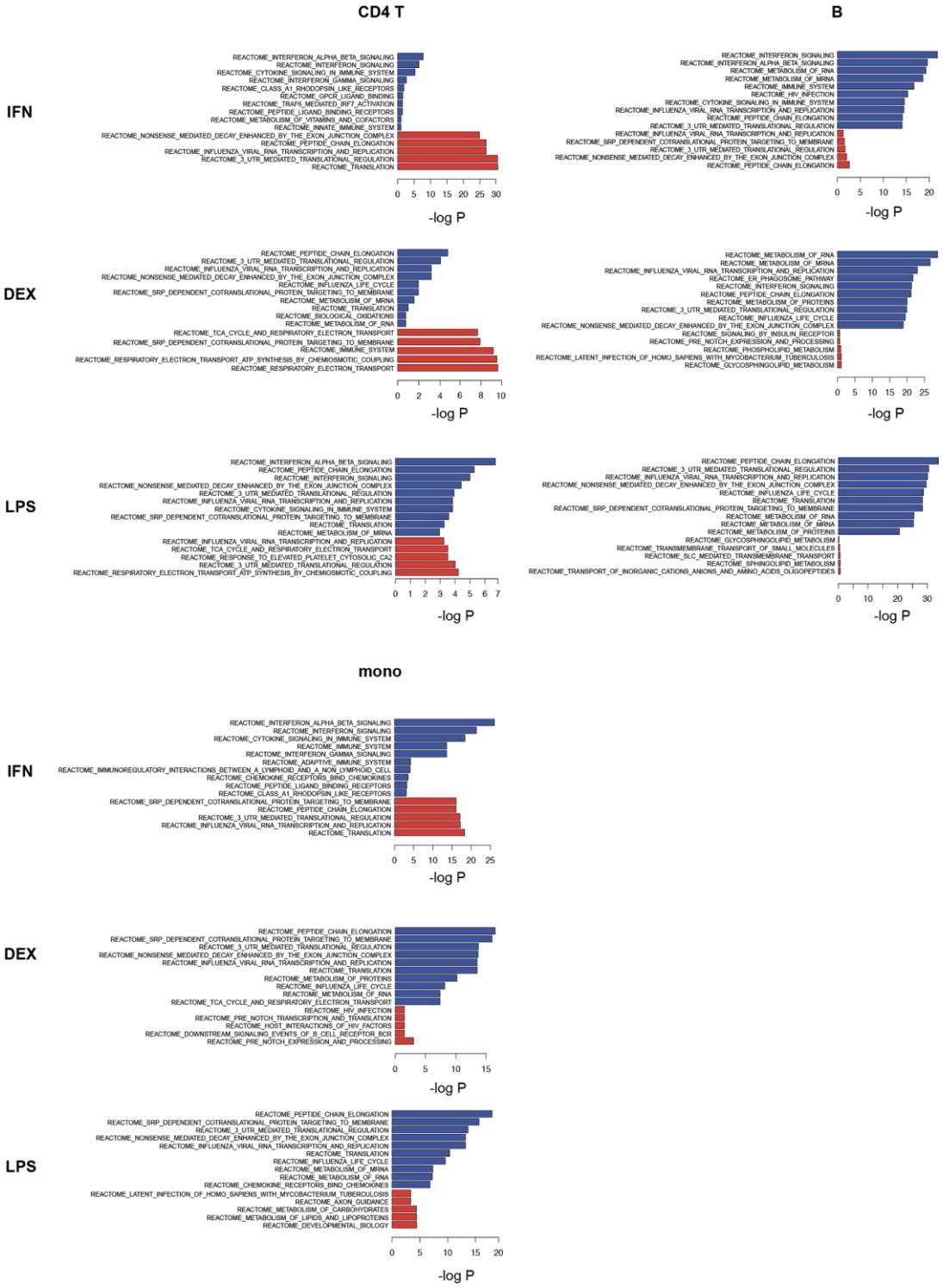

Fig. S9. Gene set enrichment analysis (Reactome sets) comparing treated PBMCs versus control. Blue bars indicated upregulated sets in treated case, while red bars indicated upregulated sets in controls. *P*-values shows are corrected for multiple gene set testing (Benjamini-Hochberg).

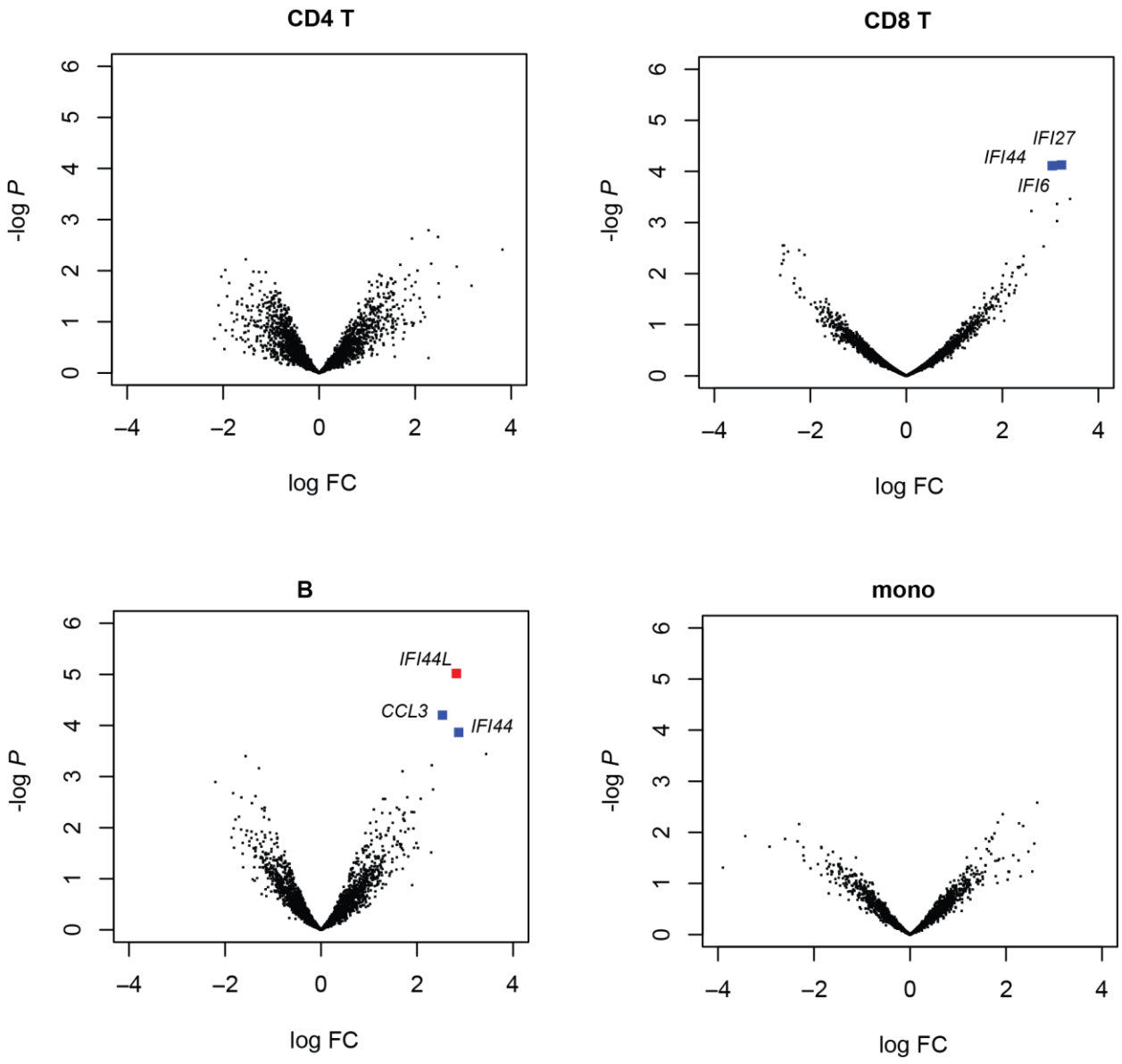

Fig. S10. Volcano plots showing differentially expressed genes between patients with SLE and matched healthy controls for four different subsets. Red points indicate genes with FDR < 0.05, while blue points indicate genes with FDR < 0.2.

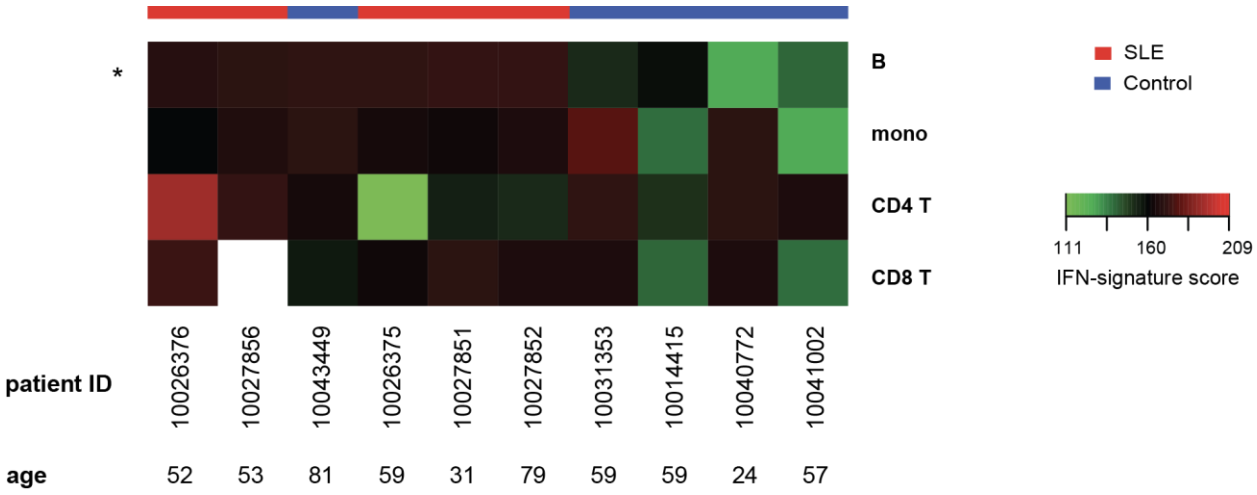

Fig. S11. Heat map showing relative IFN-signature scores across different cell types of 10 patients. Raw scores are shown with corresponding patient labels. (*) Asterisk indicates subsets where scores are significantly different ($P < 0.05$) between SLE and healthy controls.

Supplementary Note

Design Principles for Microfluidic Cell Isolation

Magnetic isolation was chosen over filter and/or flow-based methods to maintain optimal cell integrity for RNA-seq. The 4 µl rectangular chamber was designed specifically for cell isolation, to enable rapid but gentle mixing of the cells with beads. During the development of this process cell isolation was initially attempted by mixing beads and cells in rotary reactors with microvalves. However, cell integrity and viability diminished drastically when the valves were actuated in the process. To address this issue, we developed a passive mixing approach that used moving magnetic beads rather than valve actuation. Once pure cell populations are obtained, lysis and subsequent steps are performed in the rotary reactors, where maintenance of cell integrity no longer applies.

Supplementary Methods

Clinical Sample Processing

The ten clinical samples were processed in two days using four devices in parallel. Samples for patients 1004772, 10041002, 10031353, 10026376, 10027851 were processed during day 1, and the rest were processed on day 2. Sample batches were chosen such that age-matched SLE and healthy control (HC) samples were processed on the same day. For both days, the samples were thawed by incubation at 37 deg. C for 2 mins, followed by gradual addition of RPMI-1640 (Gibco), to a total of 10 mL. The cells were then spun down (300 rcf, 5 min), resuspended in 10 mL RPMI-1640, and counted. The cells were the spun down again (300 rcf, 5 min) and resuspended to the appropriate concentration.

Each device (10 lanes) was used to isolate and process one subset for 5 patients in duplicate. B cells and $CD14^+$ monocytes were isolated by positive selection for CD19 and CD14, respectively. $CD4^+$ and $CD8^+$ T cells were isolated by depletion of non-T cells and subsequent positive selection for CD4 and CD8. For both days, the PCR products from whole-transcription amplification were taken off the chip for benchtop SPRI. The products were then processed for sequencing using the protocols described for the technical validation and *in vitro* experiment samples.

Data analysis and normalization for clinical study

The RNA-seq libraries were sequenced, and alignments and expression matrices were generated using STAR and RSEM as described in the **Methods**. Libraries which showed < 7000 genes (count >=1) or had a transcript mapping rate < 50% based on RNA-SeQC were excluded from downstream analyses. Out of 80 libraries generated, 66 passed the quality filtering. Out of the 14 libraries that didn't pass the filter, 8 related to identifiable technical issues during the device processing run. After filtering, an average expression matrix was generated for each sample by taking the average count or TPM values of the two replicate libraries. For differential expression analysis using edgeR, the sample processing batch and patient-matching were included as covariates in the generalized linear model, and only the top 3000 highly expressed genes were considered. Gene set enrichment analysis was also performed on this matrix independently using the gage package.

IFN signature score

An IFN signature score was generated by removing batch effects from the TPM expression matrix using edgeR and generating a score for each sample by taking the sum of TPM values for the following genes: *IFI35, IFIT1, IFIT3, IFITM1, MX1, OAS1, STAT1, STAT2, CCL2, CXCL1, SOCS1, SOCS3, CCL3, CCR1, CD163, FCGR1A, IL1R2, IL1B, IL1RN, IL-8, NFAT5, MAP2K3, MAP2K6, SMAD3, FCGR2A, FCGR2B, NFKBIA, CDKN1C, CDK1A, DUSP1, EP300, FOS, JUN, PRKACA, PRKACB, SLP*. These genes were chosen based on a previous meta-analysis that identified a 37-gene signature score for SLE from publicly available microarray data[5].